ISSN 0030-5987. Orthopaedics, traumatology and prosthetics. 2025. № 4

УДК 617.583/.585-007.2-092.9:004.94](045)

DOI: http://dx.doi.org/10.15674/0030-59872025499-107

Degenerative changes in rat ankle cartilage induced by varus extra-articular femoral deformation

K. K. Romanenko, N. O. Ashukina, V. Ye. Maltseva

Sytenko Institute of Spine and Joint Pathology National Academy of Medical Sciences of Ukraine, Kharkiv

Objective. To evaluate the structure of ankle joint articular cartilage in rats following experimentally induced deformation of the middle third of the femur over a six-month observation period. Methods. An experimental study was conducted on 18 six-month-old male rats divided into two groups. In the experimental group, extra-articular femoral deformation was modeled by inserting a Kirschner wire fragment bent at a 35° angle into the medullary cavity; the control group remained intact. Animals were evaluated at 1, 3, and 6 months. Structural changes in the articular cartilage were assessed using the Osteoarthritis Research Society International (OARSI) scale, and the height of the articular cartilage of the ankle joint was measured. Results. At 1 month, structural changes were observed only in the talar cartilage, corresponding to OARSI grades 0–1. At 3 months, changes in the tibial cartilage corresponded to grades 1–2, in the talar cartilage to grades 1–3, and in the contralateral limb to grades 0–1 for both surfaces. At 6 months, tibial cartilage changes reached grade 2, talar cartilage grade 2–3, and the contralateral limb grade 1–2. Cartilage height in rats with deformity decreased 1.2-fold from the 3rd month ($p < 0.001$) and did not differ from the contralateral limb at 6 months. Compared with intact rats, talar and tibial cartilage height in rats with deformity also decreased from the 3rd month by 1.4-fold ($p < 0.001$) and 1.1-fold ($p = 0.022$), respectively. Conclusions. Extra-articular deformation of the middle third of the femur induces degenerative changes in talar articular cartilage beginning at 1 month, and in tibial cartilage from 3 months after modeling.

Мета. Дослідити структуру суглобового хряща надп'ятково-гомілкового суглоба після моделювання деформації середньої третини стегнової кістки в щурів протягом півроку спостереження. Методи. Експериментальне дослідження проведено на 18 щурах самцях віком 6 міс. у двох групах: перша — моделювали позасуглобову деформацію стегнової кістки шляхом введення в кістково-мозковий канал фрагмента спиці Кіршнера, вигнутого під кутом 35°, друга — інтакт. Спостереження тривало 1, 3 та 6 міс. Оцінювали структурні зміни за шкалою Osteoarthritis Research Society International (OARSI) та вимірювали висоту в суглобовому хрящі надп'ятково-гомілкового суглоба. Результати. Через місяць у щурів із деформацією стегнової кістки виявлено структурні зміни лише в суглобовому хрящі надп'яткової кістки, що відповідали 0–1 ступеням за шкалою OARSI. Через 3 міс. зміни в суглобовому хрящі великогомілкової кістки відповідали 1–2, надп'яткової — 1–3, а у контралатеральній кінцівці для обох поверхонь — 0–1 ступеням за шкалою OARSI. Через 6 міс. структурні зміни в суглобовому хрящі великогомілкової кістки оцінили як 2, надп'яткової кістки — 2–3, а у контралатеральній кінцівці — 1–2 ступені за шкалою OARSI. Висота суглобового хряща обох суглобових поверхонь у щурів із деформацією знизилася з 3-го місяця в 1,2 рази і не відрізнялася через 6 міс. ($p = 0,105$) як порівняти з контралатеральною кінцівкою. Висота суглобового хряща обох суглобових поверхонь у щурів із деформацією знизилася з 3-го місяця в 1,2 рази ($p < 0,001$) і не відрізнялася через 6 міс. у порівнянні з контралатеральною кінцівкою. Порівняно з інтактом висота суглобового хряща надп'яткової та великогомілкової кісток у щурів із деформацією також знизилася з 3-го місяця в 1,4 рази ($p < 0,001$) та 1,1 рази ($p = 0,022$) відповідно. Висновки. Змодельована позасуглобова деформація середньої третини стегнової кістки щурів викликає дегенеративні зміни в суглобовому хрящі надп'яткової кістки з першого місяця, а з третього — великогомілкової кістки в надп'ятково-гомілковому суглобі. Ключові слова. Надп'ятково-гомілковий суглоб, суглобовий хрящ, дегенерація, деформація стегнової кістки, варусна деформація, щур.

Key words. Ankle joint, Articular cartilage, Degeneration, Femoral deformity, Varus deformity, Rat model

Introduction

According to various authors, the incidence of femoral shaft fractures at the level of the middle third is approximately 10–37 cases per 100,000 population, with two age peaks (youth and elderly) [1, 2]. It has been reported that the development of post-traumatic deformities ranges from 6 to 13 % [3, 4], though this is more common when the fracture is located at the distal or proximal third of the femur [5].

Femoral shaft fractures can be associated with complications such as nonunion [6], malrotation [7], and further deformity. These complications are characterized by impaired functioning of the entire lower limb and the development of degenerative changes in the knee and hip joints as a result [8, 9]. However, a 22-year follow-up of 62 patients with post-traumatic deformities and axial alignment disturbances due to femoral shaft fractures revealed no signs of osteoarthritis in the knee joint, though mild pain was present [10].

Typically, the treatment for femoral shaft fractures is surgical, often involving the use of an intramedullary nail for fixation [11]. However, according to a Cochrane review, the use of retrograde intramedullary nails increases the risk of valgus/varus deformities in the future [12]. At the same time, it has been shown that individuals with rotational malalignment of fragments with an angle < 10° after fracture treatment can adapt to this condition and remain pain-free [13], though the chances are low if the angle of deformity exceeds 30° [7]. It has also been found that patients with similar malalignment report pain in the knee, hip, and patellofemoral joints [14, 15]. Furthermore, there is still controversy regarding whether external or internal rotational deformities cause more complications. Two clinical studies [13, 14] suggest that external rotational deformity is better tolerated, while R. L. Jaarsma et al. [16] reported a higher number of complaints from patients with this type of deformity.

Thus, most modern studies focus on rotational post-traumatic deformities of the femur rather than axial ones. This is due to differences in treatment approaches between developed countries and Ukraine. In these countries, intramedullary fixation of the femoral shaft fragments is the standard for final fixation, while in Ukraine, this is mostly done with extramedullary osteosynthesis and external fixation devices. The widespread use of the latter is explained by the specifics of treating combat-related injuries. At the same time, the widespread use of intramedullary fixation, as noted by B. Cunningham et al. [17], has significantly reduced the frequency and significance of post-traumatic deformities of the femur with axial alignment disturbances.

Displacement of the physiological axis of the lower limb due to femoral bone deformity alters the distribution of load not only on the knee joint but possibly also on the ankle joint. However, secondary osteoarthritis of the ankle joint has received little attention in both clinical [18] and experimental studies [19]. Some studies have examined the development of osteoarthritis of the ankle joint due to fractures of the calcaneus [20] and have created an experimental model based on intra-articular fractures of bones [21]. However, the possibility of complications from higher-placed fractures remains unclear. Experimentally, it has been established that non-physiological loading of the articular cartilage can lead to chondrocyte deformation [22], alter the content of proteoglycans in the cartilage matrix depending on the area of load [22], and cause microfractures under low cyclic loading [23].

Objective: To investigate the structure of the articular cartilage of the ankle joint after modeling a deformity of the femoral shaft in rats over a six-month follow-up period.

Methods

Experiments were conducted on 18 male white laboratory rats (6 months old at the start of the study), purchased from the Experimental Biology Clinic of the State Institution Professor M.I. Sytenko Institute of Spine and Joint Pathology of the National Academy of Medical Sciences of Ukraine. The study protocol was approved by the local bioethics committee (No. 117 dated 22.04.2013), in accordance with the rules of the "European Convention for the Protection of Vertebrate Animals Used for Experimental and Other Scientific Purposes" and the Law of Ukraine on the Protection of Animals from Cruelty [24, 25].

Surgical Intervention

The rats were operated on under general anesthesia (ketamine, 50 mg/kg intramuscularly) in aseptic and antiseptic conditions (Fig. 1). After preparing the surgical site with Betadine® solution, the skin was incised, and a lateral intermuscular approach was used to expose the middle third of the femoral diaphysis (Fig. 1a). A transverse osteotomy was performed using a disc saw (Fig. 1b). To model a varus deformity (9 rats), a Kirschner wire fragment was inserted into the bone marrow canal (Fig. 1g), matching its dimensions and length, and bent at an angle of 35° (Fig. 1d) [26]. A comparison group consisted of 9 intact rats of the same age and sex. After 1, 3, and

6 months post-surgery, 5 animals from each group were euthanized using a lethal dose of anesthetic (sodium thiopental, 90 mg/kg intramuscularly).

All rats underwent radiographic examination immediately after surgery (Fig. 2a).

Histological Analysis

After euthanasia, the ankle joints from both hind limbs of the rats were harvested. The fragments were fixed for 4 days in a 10 % neutral formalin solution, then decalcified in 10 % formic acid, dehydrated through a series of increasing concentrations of isopropyl alcohol (80, 90, 90, 100, 100, 100 %), infiltrated with a mixture of paraffin and isopropyl alcohol, followed by paraffin embedding. Sagittal sections, taken through the central axis of the limb, were 5–6 µm thick and stained with hematoxylin and eosin. The histological sections were analyzed using a BX53 microscope and photographed using a DP73 camera.

Structural changes in the articular cartilage covering the articular surfaces of the tibia and talus were assessed according to the general guidelines for determining cartilage damage stages, developed by the Osteoarthritis Research Society International (OARSI) for rats. A grade of 0 indicates normal cartilage, while 5 represents severe degenerative changes [27].

The total thickness of the articular cartilage (both calcified and non-calcified) on the distal end of the tibia and the proximal end of the talus was measured (Fig. 2b) using the "CellSens Dimension 1.8.1" software.

Statistical Methods

Results are presented as the mean ± standard deviation. To determine the effect of femoral shaft deformity on cartilage thickness, data comparisons were made using the Student's t-test. Comparisons between the deformed limb and contralateral limb were also conducted using the paired samples t-test. A difference was considered statistically significant if $p < 0.05$. Statistical analysis was performed using IBM SPSS Statistics 20.

Results

Histological Analysis

One month after modeling the femoral deformity, the articular surfaces in the ankle joint were congruent. The structure of the articular cartilage of the tibia corresponded to the age norm, with clear zonality. In the superficial zone, chondrocytes formed 1–2 layers in a weakly eosinophilic matrix. In the middle zone, chondrocytes with large hypochromic nuclei were evenly distributed, forming isogenic groups of 2–3 cells. The matrix was evenly stained. The basophilic line was observed across the entire surface of the articular cartilage. The calcified cartilage zone maintained a characteristic normal structure (Fig. 3a).

In the articular cartilage covering the lateral side of the talus, moderate destructive changes were detected, corresponding to grade 0–1 on the OARSI scale. Specifically, irregularities in the contours of the superficial zone were noted. At the boundary between the middle zone and the calcified cartilage, isogenic groups of 4 chondrocytes were observed (Fig. 3b). Additionally, areas without chondrocytes were noted. The matrix showed uneven staining. No structural changes were found in the articular cartilage of the contralateral ankle joint.

Three months after modeling the deformity, degenerative changes were observed in the articular cartilage of the distal end of the tibia, corresponding to 1–2 degrees on the OARSI scale. The superficial zone showed loosening, and the matrix staining was uneven. In the middle zone, some chondrocyte nuclei were hyperchromatic, and there were focal areas of matrix destruction with collagen fibers being unmasked. The basophilic line was interrupted, but the calcified cartilage zone retained its characteristic features (Fig. 4a).

In the contralateral limb, structural changes were found only in the superficial zone (Fig. 4b), corresponding to grades 0–1 on the OARSI scale.

In the articular cartilage of the talus on the deformed limb, the matrix showed uneven staining, and dead chondrocytes were present in the superficial zone. In the middle zone, chondrocytes were necrotic and had low density. The basophilic line was irregular, and in the calcified cartilage zone, focal areas of bone tissue were formed, occasionally extending to the basophilic line (Fig. 4g). Degenerative changes were graded as 1–3, while in the contralateral limb's articular cartilage, they were grade 0–1. In the contralateral limb, chondrocytes in the middle zone were disorganized, and the basophilic line was uneven (Fig. 4d).

Six months after creating the deformity, the superficial zone in the articular cartilage of the distal end of the tibia was no longer visible, and the middle zone (Fig. 5a) was significantly narrower compared to the contralateral limb (Fig. 5b) and intact limb (Fig. 5c). In this zone, the matrix was unevenly stained, and the acellular areas occupied a larger area than at the previous time point. The basophilic line was intermittently absent, and the calcified cartilage zone had widened nearly twice as much as the middle zone (Fig. 5a).

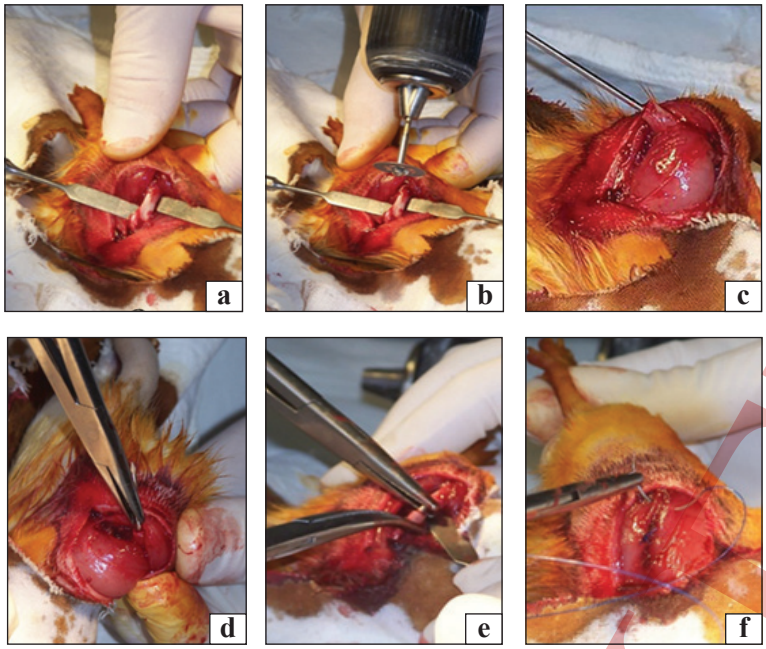

Fig. 1. Stages of performing the surgical procedure for modeling femoral deformity in rats. The middle third of the diaphysis of the bone (a); transverse osteotomy (b); insertion of a Kirschner pin fragment into the bone marrow canal (c); bending the Kirschner pin at a 35° angle (d); applying sutures (e).

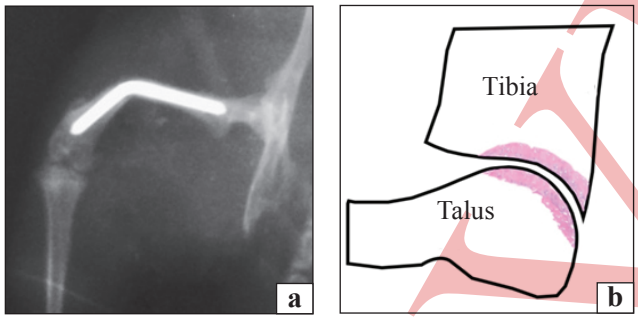

Fig. 2. Radiographic image of a rat with a limb with a modeled femoral deformity (a). Schematic representation of the articular cartilage of the talocrural joint (b).

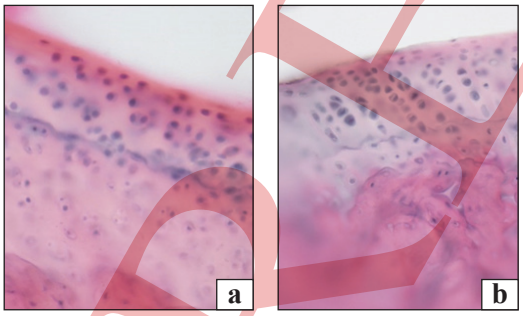

Fig. 3. Articular cartilage of the tibia (a) and talus (b) in the talocrural joint of a rat 1 month after modeled femoral deformity. Fibrillation of the surface zone of the talus articular cartilage (b). Staining with hematoxylin and eosin. Magnification 400x.

In the contralateral limb, acellular areas were detected in the middle zone, and the calcified cartilage zone was narrower compared to the intact limb (Fig. 5b). In the superficial zone of the articular cartilage of the intact limb, a decrease in chondrocyte density in the middle zone was also observed, characteristic of the age norm for rats (12 months). According to the OARSI scale, the structural changes in the deformed limb corresponded to grade 2, grade 1–2 in the contralateral limb, and grade 0–1 in the intact animals.

On the surface of the talus bone, the articular cartilage, 6 months after the femoral deformity, showed significant structural changes compared to the distal end of the tibia. The characteristic zonality was lost. There was observed delamination of the superficial zone, significant areas without cells or with chondrocytes in a state of necrosis and necrobiotic changes. The basophilic line was either completely absent or sharply basophilic. The calcified cartilage zone was very narrow and almost devoid of cells (Figure 5d). In the contralateral limb, the middle zone showed low chondrocyte density (Figure 5e). In the articular cartilage of the intact rats, the characteristic zonality was preserved with a reduction in the width of the calcified cartilage zone (Figure 5f), which was related to the age of the animals (12 months). According to the OARSI scale, the structural changes corresponded to the following: 2–3 degrees for the deformed limb, 1–2 degrees for the contralateral limb, and 0–1 degrees for the intact rats.

Histomorphometry

In the limbs of animals with deformed bones, the height of the articular cartilage of the talus and tibia was 1.2 times (60.23 ± 7.14 vs. 49.23 ± 7.70 μm; $p < 0.001$) and 1.4 times (66.14 ± 13.64 vs. 48.09 ± 9.48 μm; $p < 0.001$) greater at 1 month, 1.2 times smaller at 3 months (43.55 ± 5.30 vs.

53.50 ± 8.65 μm; 46.84 ± 7.09 vs. 57.53 ± 6.27 μm; $p < 0.001$), and did not differ at 6 months (54.51 ± 10.18 vs. 53.46 ± 5.44 μm; $p = 0.570$; 58.28 ± 10.08 vs. 55.16 ± 8.50 μm; $p = 0.105$) when compared to the contralateral limb, respectively (Figure 6).

Compared to the intact rats, the height of the articular cartilage of the talus and tibia was greater by 1.2 and 1.3 times at 1 month (47.39 ± 5.88 μm; 55.03 ± 6.98 μm; $p < 0.001$), smaller by 1.4 times (59.39 ± 8.16 μm; $p < 0.001$) and 1.1 times (53.47 ± 5.84 μm; $p = 0.022$) at 3 months, smaller by 1.1 times (61.82 ± 10.60 μm; $p < 0.001$) for the talus, but did not differ for the tibia (60.82 ± 10.08 μm; $p = 0.178$) at 6 months (Figure 6).

In the contralateral limb of rats with femoral deformity, compared to intact animals, the height of the articular cartilage of the talus did not differ at 1 month, was smaller by 1.1 times ($p = 0.018$) at 3 months, and smaller by 1.2 times ($p < 0.001$) at 6 months. The tibia cartilage was smaller by 1.1 times ($p = 0.006$) at 1 month, larger by 1.1 times ($p = 0.023$) at 3 months, and smaller by 1.1 times ($p = 0.005$) at 6 months (Figure 6).

Discussion

In the conducted experimental study, we demonstrated that extra-articular femoral deformity leads to degenerative changes in the articular cartilage of the talocrural joint in rats. However, the severity of these changes is less pronounced compared to the knee joint, which we had previously studied [28]. In the articular cartilage of the talus, structural changes began earlier than at the distal end of the tibia. Already one month after the deformity, these changes corresponded to 0–1 degrees on the OARSI scale [27]. Degenerative changes progressed over time and reached 2–3 degrees after 6 months of observation. In the articular cartilage at the distal end of the tibia, destructive changes were observed later, starting from 3 months of observation, but their degree of manifestation was similar after 6 months, as in the talus bone. The height of the articular cartilage on both surfaces at the first month of observation was higher compared to the contralateral limb and intact animals, but by 3 months, it became smaller, and at 6 months, it was smaller only for the talus surface. These changes align with structural alterations that progressed more in the talus of the limb with deformity. At the same time, the likely increased height of the articular cartilage at the first month of observation is associated with a reduction in load on the limb due to the injury.

Degenerative changes in the articular cartilage, leading to osteoarthritis, begin in the superficial zone, followed by the loss of its distinct contour and chondrocyte death. One of the factors contributing to this is impaired biomechanics/instability, either due to post-traumatic osteoarthritis or excessive loads in obesity [29]. In the model of femoral deformity, we believe that an abnormal load distribution on the limb and talocrural joint also occurs. We observed the development of degenerative changes more on the side of the articular cartilage surface than in the calcified zone, which is characteristic of excessive loading, rather than aging [29].

By the end of the observation period, delamination of part of the superficial zone was detected, indicating chondrocyte death, which secretes matrix components, and subsequent cracking of the matrix. S. Santos et al. [23] showed that mechanical loading induces microcracks in the collagen network of articular cartilage samples.

The biomechanics of the hind limbs of rats differ from those of humans, which may influence the development of osteoarthritis, and this needs to be considered. However, S. H. Chang et al. [30] found no differences when comparing structural changes in the talocrural joint in three mouse models of osteoarthritis with human samples. It remains unknown how this applies to the talocrural joint in rats. Currently, there is little information regarding the condition of the talocrural joint in patients with extra-articular femoral deformity [8, 15]. Clinical studies typically focus on the knee joint [7, 10], where biomechanical changes closer to the defect lead to more pronounced alterations and osteoarthritis development. But biomechanically, it has been shown that axial alignment disturbances in femoral fragments after surgical treatment of a fracture lead to excessive loading on the talocrural joint [14]. We obtained similar results in a previously conducted study, where we modeled femoral deformity and found an increase in maximal stress on the articular surfaces [31]. However, there is a lack of clinical observations regarding osteoarthritis development in the talocrural joint in individuals with femoral deformity [18]. This may be due to the fact that degenerative changes in this location in such patients do not cause significant pain or noticeable functional impairment, especially when compared to the knee joint. Additionally, pain in osteoarthritis, according to recent data, is not associated with damage to the articular cartilage, which lacks nerve endings [32]. This disease in the early stages in the talocrural joint can be effectively controlled with therapy using non-steroidal anti-inflammatory drugs [33].

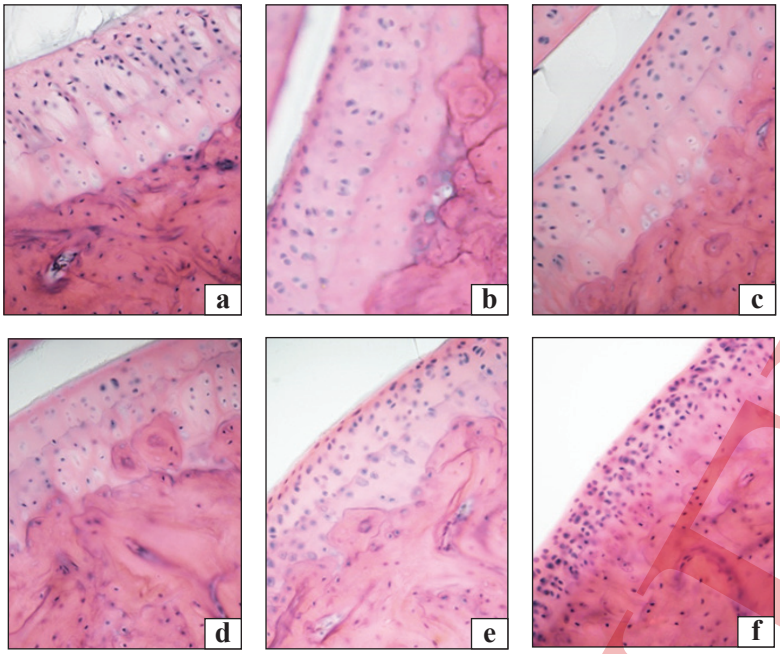

Fig. 4. Articular cartilage of the tibia (top row) and talus (bottom row) in the talocrural joint of rats 3 months after modeling femoral deformity (a, d), compared with the contralateral limb (b, e) and intact (c, f). Disruption of histoarchitecture (a), areas without cells, cells in a state of necrobiosis, uneven matrix staining (d) after deformity. Moderate disruption of cartilage histoarchitecture in the contralateral limb (b, e). Staining with hematoxylin and eosin. Magnification 400x.

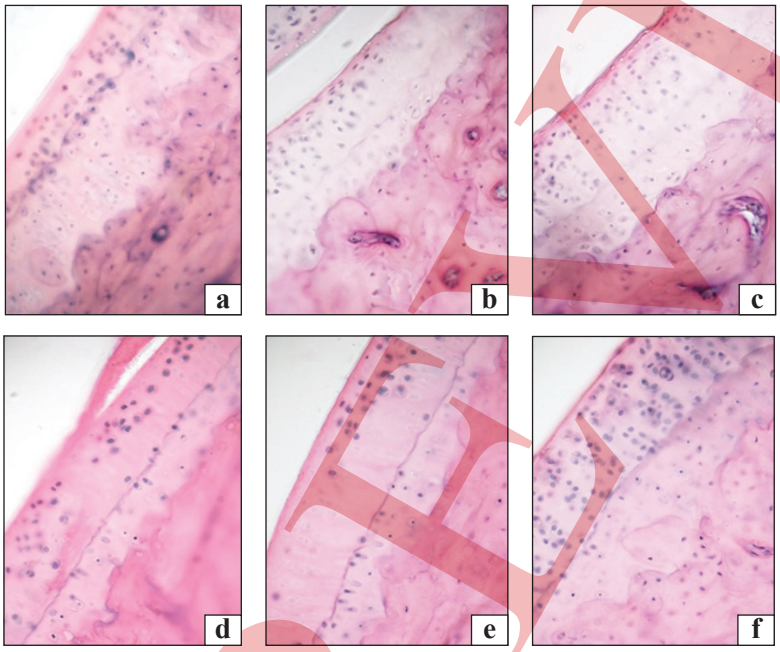

Fig. 5. Articular cartilage of the tibia (top row) and talus (bottom row) in the talocrural joint of rats 3 months after modeling femoral deformity (a, d), compared with the contralateral limb (b, e) and intact (c, f). Narrow middle zone with sparsely located chondrocytes, uneven matrix staining (a), detachment of the surface zone (d) after deformity. Disruption of the histoarchitecture of the articular cartilage, areas without cells (b, e).

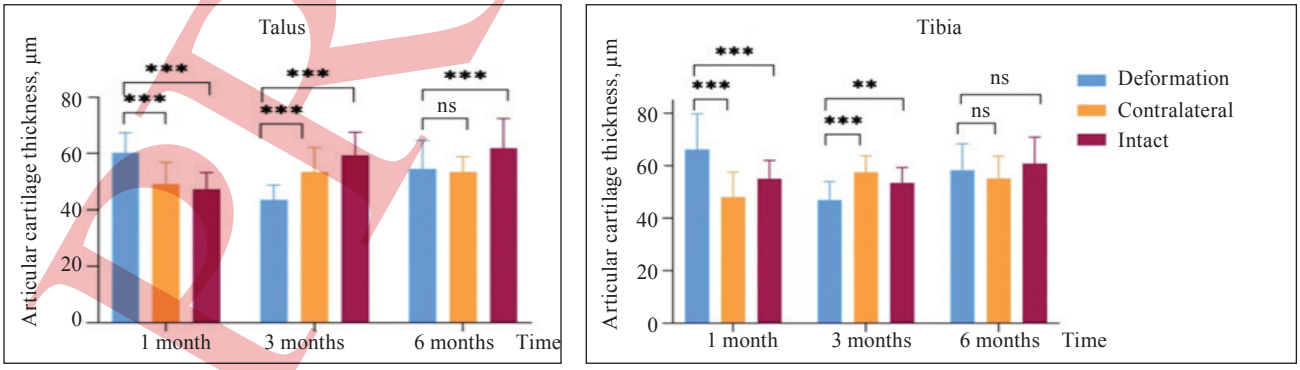

Fig. 6. Comparison of articular cartilage thickness of the distal tibia and proximal talus in the limbs of rats with femoral deformity versus the contralateral limb and the intact group of rats. Notation: ** $p < 0.01$; *** $p < 0.001$; ns — no differences.

However, femoral deformity causes systemic changes in the axis of the limb that affect the function of all its joints [14], and likely even in the contralateral limb, as we demonstrated in the articular cartilage of the distal end of the tibia in the contralateral limb of rats after 3 months of observation. This highlights the importance of comprehensive examination of patients with bone deformities to develop preventive measures aimed at preserving the function of the joints in both limbs.

An interesting aspect is the development of degenerative changes initially in the articular cartilage of the talus in the talocrural joint of rats. This may be linked to the greater load on the bones of the foot during walking and their function of absorbing the load, in contrast to the long bones, where the load transmitted is already of lesser force by the time of the first contact with the surface. This is confirmed by biomechanical studies on post-mortem limb specimens, which showed that ≈ 83% of the load is borne by the articular cartilage of the talus in this joint [34].

When evaluating the risk of osteoarthritis development in the talocrural joint, it is important to take into account the age of patients with extra-articular femoral deformity and the duration of the deformity. In our experimental study, we used rats aged 6 months because, according to leading experimental researchers' recommendations [27], degenerative changes do not develop in younger animals under osteoarthritis modeling. Therefore, it is likely that in younger patients, changes in the talocrural joint will be less pronounced and will not interfere with normal physical activity.

A limitation of this study is the examination of structural changes in the articular cartilage using sagittal sections taken through the central axis of the rat limb, whereas the load on the medial part of the cartilage may have been higher due to the varus deformity. At the same time, the degenerative changes observed even under these conditions suggest that the deformity affects even the less-loaded areas of the joint.

Conclusion

The modeled extra-articular femoral deformity in rats induces degenerative changes in the articular cartilage of the talus from the first month, and from the third month, in the tibia in the talocrural joint. In the contralateral limb, degenerative changes in the articular cartilage were observed after 3 months, but they were less pronounced.

Conflict of Interest. The authors declare no conflict of interest.

Future Research Prospects. Further experimental modeling of valgus deformity in the mid-third of the femur followed by studies on the articular cartilage structure in the knee and talocrural joints.

Funding Information. The study was conducted within the framework of the scientific research project "Study of pathological changes in the joints of the lower limbs under post-traumatic extra-articular deformities in adults", State registration number 0114U003020.

Author Contributions. Romanenko K. K. — Concept and design, experimental modeling in rats, editing and approval of the final version of the article; Ashukina N. O. — Experimental modeling in rats, histological analysis, drafting the article; Maltseva V. Ye. — Data analysis, data visualization, approval of the final version of the article.

References

1. Weiss, R. J., Montgomery, S. M., Al Dabbagh, Z., & Jansson, K. Å. (2009). National data of 6409 Swedish inpatients with femoral shaft fractures: Stable incidence between 1998 and 2004. *Injury, 40*(3), 304–308. https://doi.org/10.1016/j.injury.2008.07.017
2. Arneson, T. J., Melton, L. J., Lewallen, D. G., & O'Fallon, W. M. (1988). Epidemiology of diaphyseal and distal femoral fractures in Rochester, Minnesota, 1965–1984. *Clinical orthopaedics and related research,* 234, 188–194. https://doi.org/10.1097/00003086-198809000-00033
3. Böstman, O., Varjonen, L., Vainionpä, S., Majolä, A., & Rokkanen, P. (1989). Incidence of local complications after intramedullary nailing and after plate fixation of femoral shaft fractures. *Journal of trauma - injury, infection and critical care, 29*(5), 639–645. https://doi.org/10.1097/00005373-198905000-00019
4. Ricci, W. M., Bellabarba, C., Evanoff, B., Herscovici, D., DiPasquale, T., & Sanders, R. (2001). Retrograde versus antegrade nailing of femoral shaft fractures. *Journal of orthopaedic trauma, 15*(3), 161–169. https://doi.org/10.1097/00005131-200103000-00003
5. Ricci, W. M., Bellabarba, C., Lewis, R., Evanoff, B., Herscovici, D., DiPasquale, T., & Sanders, R. (2001). Angular malalignment after intramedullary nailing of femoral shaft fractures. *Journal of orthopaedic trauma, 15*(2), 90–95. https://doi.org/10.1097/00005131-200102000-00003
6. Jensen, S. S., Jensen, N. M., Gundtoft, P. H., Kold, S., Zura, R., & Viberg, B. (2022). Risk factors for nonunion following surgically managed, traumatic, diaphyseal fractures: a systematic review and meta-analysis. *EFORT open reviews, 7*(7), 516–525. https://doi.org/10.1530/EOR-21-0137
7. Vergano, L. B., Coviello, G., & Monesi, M. (2020). Rotational malalignment in femoral nailing: Prevention, diagnosis and surgical correction. *Acta biomedica, 91*(Suppl 14), 1–11. https://doi.org/10.23750/abm.v91i14-S.10725
8. Eckhoff, D. G. (1994). Effect of limb malrotation on malalignment and osteoarthritis. *Orthopedic clinics of North America, 25*(3), 405–414. https://doi.org/10.1016/s0030-5898(20)31925-8
9. Castano Betancourt, M. C., Maia, C. R., Munhoz, M., Morais, C. L., & Machado, E. G. (2022). A review of Risk Factors for Post-traumatic hip and knee osteoarthritis following musculoskeletal injuries other than anterior cruciate ligament rupture. *Orthopedic reviews, 14*(4), 2022. https://doi.org/10.52965/001c.38747
10. Phillips, J. R. A., Trezies, A. J. H., & Davis, T. R. C. (2011). Long-term follow-up of femoral shaft fracture: Relevance of malunion and malalignment for the development of knee arthritis. *Injury, 42*(2), 156–161. https://doi.org/10.1016/j.injury.2010.06.024
11. Ricci, W. M., Gallagher, B., & Haidukewych, G. J. (2009). Intramedullary nailing of femoral shaft fractures: Current

concepts. *Journal of the American academy of orthopaedic surgeons, 17*(5), 296–305. https://doi.org/10.5435/00124635-200905000-00004
12. Claireaux, H. A., Searle, H. K. C., Parsons, N. R., & Griffin, X. L. (2022). Interventions for treating fractures of the distal femur in adults. *Cochrane database of systematic reviews, 2022*(10). https://doi.org/10.1002/14651858.CD010606.pub3
13. Gugala, Z., Qaisi, Y. T., Hipp, J. A., & Lindsey, R. W. (2011). Long-term functional implications of the iatrogenic rotational malalignment of healed diaphyseal femur fractures following intramedullary nailing. *Clinical biomechanics, 26*(3), 274–277. https://doi.org/10.1016/j.clinbiomech.2010.11.005
14. Dagneaux, L., Allal, R., Pithioux, M., Chabrand, P., Ollivier, M., & Argenson, J.-N. (2018). Femoral malrotation from diaphyseal fractures results in changes in patellofemoral alignment and higher patellofemoral stress from a finite element model study. *The knee, 25*(5), 807–813. https://doi.org/10.1016/j.knee.2018.06.008
15. Karaman, O., Ayhan, E., Kesmezacar, H., Seker, A., Unlu, M. C., & Aydingoz, O. (2014). Rotational malalignment after closed intramedullary nailing of femoral shaft fractures and its influence on daily life. *European journal of orthopaedic surgery and traumatology, 24*(7), 1243–1247. https://doi.org/10.1007/s00590-013-1289-8
16. Jaarsma, R. L., Ongkiehong, B. F., Grüneberg, C., Verdonschot, N., Duysens, J., & Van Kampen, A. (2004). Compensation for rotational malalignment after intramedullary nailing for femoral shaft fractures: An analysis by plantar pressure measurements during gait. *Injury, 35*(12), 1270–1278. https://doi.org/10.1016/j.injury.2004.01.016
17. Cunningham, B. P., Cole, P. A., & Ortega, G. (2020). *Malunions of the Femoral Shaft. In Malunions: Diagnosis, Evaluation and Management* (261–282). Springer, New York, NY. https://doi.org/10.1007/978-1-0716-1124-1_10
18. Kim, J. S., Amendola, A., Barg, A., Baumhauer, J., Brodsky, J. W., Cushman, D. M., Gonzalez, T. A., Janisse, D., Jurynec, M. J., Lawrence Marsh, J., Sofka, C. M., Clanton, T. O., & Anderson, D. D. (2022). Summary report of the arthritis foundation and the american orthopaedic foot & ankle society's symposium on targets for osteoarthritis research: part 1: epidemiology, pathophysiology, and current imaging approaches. *Foot and ankle orthopaedics, 7*(4). https://doi.org/10.1177/24730114221127011
19. Delco, M. L., Kennedy, J. G., Bonassar, L. J., & Fortier, L. A. (2017). Post-traumatic osteoarthritis of the ankle: A distinct clinical entity requiring new research approaches. *Journal of orthopaedic research, 35*(3), 440–453. https://doi.org/10.1002/jor.23462
20. Godoy-Santos, A. L., Fonseca, L. F., de Cesar Netto, C., Giordano, V., Valderrabano, V., & Rammelt, S. (2021). Ankle osteoarthritis. *Revista Brasileira de ortopedia, 56*(6), 689–696. https://doi.org/10.1055/s-0040-1709733
21. Liang, D., Sun, J., Wei, F., Zhang, J., Li, P., Xu, Y., Shang, X., Deng, J., Zhao, T., & Wei, L. (2017). Establishment of rat ankle post-traumatic osteoarthritis model induced by malleolus fracture. *BMC musculoskeletal disorders, 18*(1). https://doi.org/10.1186/s12891-017-1821-9
22. Guo, J. B., Liang, T., Che, Y. J., Yang, H. L., & Luo, Z. P. (2020). Structure and mechanical properties of high-weight-bearing and low-weight-bearing areas of hip cartilage at the micro- And nano-levels. *BMC musculoskeletal disorders, 21*(1). https://doi.org/10.1186/s12891-020-03468-y
23. Santos, S., Emery, N., Neu, C. P., & Pierce, D. M. (2019). Propagation of microcracks in collagen networks of cartilage under mechanical loads. *Osteoarthritis and cartilage, 27*(9), 1392–1402. https://doi.org/10.1016/j.joca.2019.04.017
24. European convention for the protection of vertebrate animalsused for experimental and other scientific purposes: Strasbourg,18 March 1986. (2000).
25. Law of Ukraine No. 3447-IV, article 26. On the protection of animals from cruel treatment. Kyiv, 21 February, 2006. (In Ukrainian)
26. Romanenko, K. K., Ashukina, N. O., Goridova, L. D., & Prozorovsky, D. V. (2014). Method for modeling fractures of long bones of limbs (92613). https://base.nipo.gov.ua/searchbulletin/search.php?action=viewdetails&dbname=invdu&IdClaim=203923
27. Gerwin, N., Bendele, A., Glasson, S., & Carlson, C. (2010). The OARSI histopathology initiative — recommendations for histological assessments of osteoarthritis in the rat. *Osteoarthritis and cartilage*, 18, S24–S34. https://doi.org/10.1016/j.joca.2010.05.030
28. Romanenko, K., Ashukina, N., Batura, I., & Prozorovsky, D. (2017). Morphology of the articular cartilage of the knee joint in rats with extraarticular femoral bone deformity. *Orthopaedics, traumatology and prosthetics, 0*(1), 63–71. https://doi.org/10.15674/0030-59872017163-71
29. Yao, Q., Wu, X., Tao, C., Gong, W., Chen, M., Qu, M., Zhong, Y., He, T., Chen, S., & Xiao, G. (2023). Osteoarthritis: Pathogenic signaling pathways and therapeutic targets. *Signal transduction and targeted therapy, 8*(1). https://doi.org/10.1038/s41392-023-01330-w
30. Chang, S. H., Yasui, T., Taketomi, S., Matsumoto, T., Kim-Kaneyama, J. R., Omiya, T., Hosaka, Y., Inui, H., Omata, Y., Yamagami, R., Mori, D., Yano, F., Chung, U., Tanaka, S., & Saito, T. (2016). Comparison of mouse and human ankles and establishment of mouse ankle osteoarthritis models by surgically-induced instability. *Osteoarthritis and cartilage, 24*(4), 688–697. https://doi.org/10.1016/j.joca.2015.11.008
31. Korzh, M., Romanenko, K., Karpinsky, M., Prozorovsky, D., & Yaresko, O. (2015). Mathematic modeling of the influence of femur malalignment on the bearing of lower extremity joints. *Orthopaedics, traumatology and prosthetics, 0*(4), 25. https://doi.org/10.15674/0030-59872015425-30
32. Tong, L., Yu, H., Huang, X., Shen, J., Xiao, G., Chen, L., Wang, H., Xing, L., & Chen, D. (2022). Current understanding of osteoarthritis pathogenesis and relevant new approaches. *Bone research, 10*(1), 1–17. https://doi.org/10.1038/s41413-022-00226-9
33. Herrera-Pérez, M., Valderrabano, V., Godoy-Santos, A. L., de César Netto, C., González-Martín, D., & Tejero, S. (2022). Ankle osteoarthritis: comprehensive review and treatment algorithm proposal. *EFORT open reviews, 7*(7), 448–459. https://doi.org/10.1530/EOR-21-0117
34. Calhoun, J. H., Li, F., Ledbetter, B. R., & Viegas, S. F. (1994). A comprehensive study of pressure distribution in the ankle joint with inversion and eversion. *Foot & ankle international, 15*(3), 125–133. https://doi.org/10.1177/107110079401500307

ISSN 0030-5987. Orthopaedics, traumatology and prosthetics. 2025. № 4

The article has been sent to the editors	Received after review	Accepted for printing
03.09.2025	14.10.2025	20.10.2025

DEGENERATIVE CHANGES IN RAT ANKLE CARTILAGE INDUCED BY VARUS EXTRA-ARTICULAR FEMORAL DEFORMATION

K. K. Romanenko, N. O. Ashukina, V. Ye. Maltseva

Sytenko Institute of Spine and Joint Pathology National Academy of Medical Sciences of Ukraine, Kharkiv

✉ Kostiantyn Romanenko, MD, PhD in Traumatology and Orthopaedics: konstantin.romanenko@gmail.com

✉ Nataliya Ashukina, PhD in Biol. Sci.: natalya.ashukina@gmail.com

✉ Valentyna Maltseva, Phd in Biol. Sci.: maltseva.val.evg@gmail.com